

ANALYSIS OF MOISTURE AND TEMPERATURE FIELDS COUPLING PROCESS IN FREEZING SHAFT

by

Yugui YANG^{a,b}, Dawei LEI^b, Haibing CAI^c, Songhe WANG^d, Yanhu MU^e*

^a State Key Laboratory for Geomechanics and Deep Underground Engineering, China
University of Mining and Technology, Jiangsu, 221116, China;

^b School of Mechanics and Civil Engineering, China University of Mining and Technology,
Jiangsu, 221116, China;

^c School of Civil Engineering and Architecture, Anhui University of Science and
Technology, Huainan, Anhui, 232001, China;

^d Institute of Geotechnical Engineering, Xi'an University of Technology, Xi'an, Shanxi,
710048, China;

^e State Key Laboratory of Frozen Soil Engineering, Northwest Institute of
Eco-Environment and Resources, Lanzhou, 730000, China

The temperature change of frozen soil wall and the evolution characteristics of the specific heat capacity are analyzed. The frozen soil cylinders form surrounding freezing pipes at initial freezing stage, and the temperature field of frozen soil presents a nonlinear decrease. With the increase of freezing time, the radius of the frozen soil cylinder increases and a frozen soil wall is enclosed. After freezing 30 days, the thickness of the frozen soil wall is obtained as 1.7m. After freezing 250 days, the thickness of frozen soil wall increases to about 11.0m.

Key words: unfrozen water, frozen soil wall, temperature field, shaft

Introduction

The artificial freezing method is one of the main construction means to pass through the thick alluvium [1]. A number of vertical freezing pipes are placed at the stratum of shaft. The freezing pipes are used to resist ground and water pressure, and prevent the collapse of shaft lining structure. The frozen soil wall can fully cut off the seepage of groundwater and offer a watertight working environment. This can improve the strength and deformation resistance ability of ground for excavation [2,3].

The artificial ground freezing technique is the best way for shaft sinking [4]. The temperature field of frozen soil wall, which is a transient evolution process with phase change, is the most important factor in freezing shaft engineering. The mechanical behavior of frozen soil is greatly affected by the temperature. The change of temperature will cause variations of mechanical properties of frozen soil, which will not be conducive to the mechanical state

control of the frozen soil wall [5]. In recent years, research has been conducted on the theory, experiment and simulation of frozen soil wall [6-10].

In fact, the temperature field of artificial frozen soil wall is greatly influenced by the unfrozen water content [11]. In order to consider the effect of unfrozen water, a discrete phase change model of temperature field around a single freezing pipe was established [12]. However, it is still urgent to study the temperature field of frozen soil wall with double or even more cycles of freezing pipes. In this paper, the temperature field with three cycles of freezing pipes is studied with the finite element method. The evolution characteristics of the temperature field and unfrozen water content are analyzed.

The governing differential equations

The coupling relationship between water and heat in frozen soil is induced by the phase change of unfrozen water. Considering the influence of phase change, a coupling equation can be given in Eq. (1) for soil materials [13]:

$$\bar{C} \frac{\partial T}{\partial t} = \frac{\partial}{\partial x} \left(\bar{\lambda} \frac{\partial T}{\partial x} \right) + \frac{\partial}{\partial y} \left(\bar{\lambda} \frac{\partial T}{\partial y} \right) + \frac{\partial}{\partial z} \left(\bar{\lambda} \frac{\partial T}{\partial z} \right) + L \rho_i \frac{\partial \theta_i}{\partial t} \quad (1)$$

where \bar{C} is the heat capacity, $\bar{\lambda}$ is the thermal conductivity, θ_i is the ice content, ρ_i is the density of ice, and L is the latent heat of phase change.

Unfrozen water content is independent of total water content and affected only by temperature when the freezing point is reached [14]. For transient thermal conduction problem, the following equation can be obtained:

$$\frac{\partial \theta_i}{\partial t} = \frac{\partial \theta_i}{\partial T} \frac{\partial T}{\partial t} \quad (2)$$

The nonlinear characteristics of the heat capacity and thermal conductivity are induced by the variation of unfrozen water content in frozen soil. The temperature parameters of frozen soil are related to the physical properties of soil particle, water and ice. The heat capacity of soil in freezing process can be expressed in terms of soil particle, water and ice contents:

$$\bar{C} = C_s \theta_s + C_w \theta_w + C_i \theta_i \quad (3)$$

where θ_s is the content of soil particles, θ_w is the content of water, θ_i is the content of ice, C_s is the specific heat of soil particles, C_w is the specific heat of water, and C_i is the specific heat of ice.

The thermal conductivity of soil in freezing process can be expressed as follows:

$$\bar{\lambda} = \lambda_s^{\theta_s} \lambda_w^{\theta_w} \lambda_i^{\theta_i} \quad (4)$$

where λ_s is the thermal conductivity of soil particle, λ_w is the thermal conductivity of water, and λ_i is the thermal conductivity of ice.

The initial temperature of differential equations at $t=0$ is determined by earth temperature, and it can be given as:

$$T|_{t=0} = T_0 \quad (5)$$

The boundary temperatures of calculating model surrounding frozen pipes are as follows:

$$T|_{\rho=\rho_0} = T_c \quad (6)$$

The remote boundary condition of the calculating model is given as:

$$T|_{\rho=\infty} = T_0 \quad (7)$$

In order to solve the governing equations mentioned above, the Galerkin method is used to deduce the finite element formulae of the temperature field for frozen soil wall. The following equation can be given:

$$[K]\{T\} + [N]\left\{\frac{\partial T}{\partial t}\right\} = \{P\} \quad (8)$$

where $[K]$ is the heat conduction matrix, $[N]$ is the heat capacity matrix, $\{T\}$ is the column matrix of temperature, and the $\{P\}$ is the column matrix of temperature load.

The components of the heat capacity matrix and heat conduction matrix are as follows:

$$N_{ij} = \sum_{\Omega} C \Phi_i \Phi_j d\Omega \quad (9)$$

$$K_{ij}^e = \sum_{\Omega^e} \bar{\lambda} \left\{ \frac{\partial \Phi_i}{\partial x} \frac{\partial \Phi_j}{\partial x} + \frac{\partial \Phi_i}{\partial y} \frac{\partial \Phi_j}{\partial y} + \frac{\partial \Phi_i}{\partial z} \frac{\partial \Phi_j}{\partial z} \right\} d\Omega \quad (10)$$

The difference method is adopted for iteration to solve the heat transfer problem, and Eq. (9) can be written as [5]:

$$\left([K] + \frac{[N]}{\Delta t} \right) \{T\}_t = \{P\}_t + \frac{[N]}{\Delta t} \{T\}_{t-\Delta t} \quad (11)$$

The unfrozen water content of frozen soil

The latent heat of water is released due to the transition from water to ice. The unfrozen water content of soils is important for the thermal computations relating to freezing or thawing [15]. The unfrozen water content of frozen soil is closely related to the temperature during freezing process [16, 17]. The amount of unfrozen water is mainly dependent on temperature, instead of the water content. The unfrozen water content of frozen soil decreases slowly with the decrease of temperature when the temperature is below the main phase change range. There is a dynamic balance between unfrozen water content and ice at a certain temperature. The relationship between the unfrozen water content and temperature is shown in Fig.1.

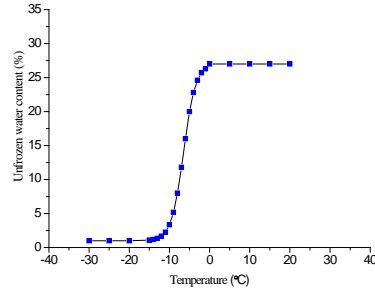


Fig.1 The relationship between unfrozen water content and temperature

The unfrozen water content can be regarded as a function of temperature. The relationship between unfrozen water content and temperature can be expressed as:

$$\theta_u(T) = a \tanh [b(T + c)] + d \quad (12)$$

where a, b, c and d are coefficients, $a = -0.13$, $b = -0.33$, $c = 6.5$ and $d = 0.14$.

Numerical simulation model and results

Project background

The depth of overburden is large in this mining area and the freezing depth of the shaft reaches about 650m, which causes the great difficulty for the construction of shaft lining. The design plans of freezing pipes are located at $R_1=7.5\text{m}$, $R_2=10.5\text{m}$, and $R_3=13.5\text{m}$, respectively. The numbers of freezing pipes for every cycle are 18, 44, and 46 respectively. The coefficients of thermal conductivities for soil particle, water and ice are $\lambda_s = 2.45\text{W}/(\text{m}\cdot^\circ\text{C})$, $\lambda_w = 0.54 \text{ W}/(\text{m}\cdot^\circ\text{C})$, and $\lambda_i = 2.22 \text{ W}/(\text{m}\cdot^\circ\text{C})$, respectively. The specific heat capacities for soil particle, water and ice are $C_s = 0.84 \text{ KJ}/(\text{kg}\cdot^\circ\text{C})$, $C_w = 4.3 \text{ KJ}/(\text{kg}\cdot^\circ\text{C})$ and $C_i = 2.1 \text{ KJ}/(\text{kg}\cdot^\circ\text{C})$. The ground temperature is about 30°C at the depth of 600m. The layout of freezing pipes and the finite element model are shown in Fig.2 and Fig.3, respectively.

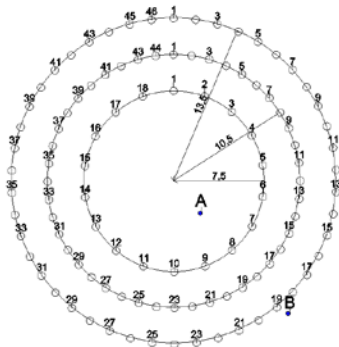


Fig.2 Layout of the freezing pipes

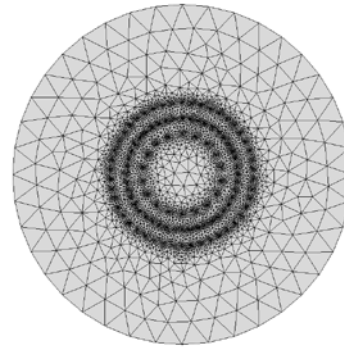


Fig.3 Finite element model of the freezing shaft

Result and analysis

The temperature field distributions of shaft at different freezing time are shown in Fig.4. The frozen cylinders surrounding the freezing pipes are formed at the beginning of freezing. The temperature of freezing soil decreases with the increase of distance from the freezing pipe. The radius of frozen cylinder continuously increases with the increase of

freezing time. Then the frozen cylinders in every freezing cycle begin to overlap and a closed frozen soil wall is formed. Fig. 5 shows the distribution of unfrozen water content at different freezing durations. The distribution of unfrozen water content is greatly affected by the freezing front. The unfrozen water content has a big difference between frozen and unfrozen regions in freezing process. There is an obvious change at the freezing front. When the temperature is below the low limit of phase change, the distribution of unfrozen water content reaches a relative stability state.

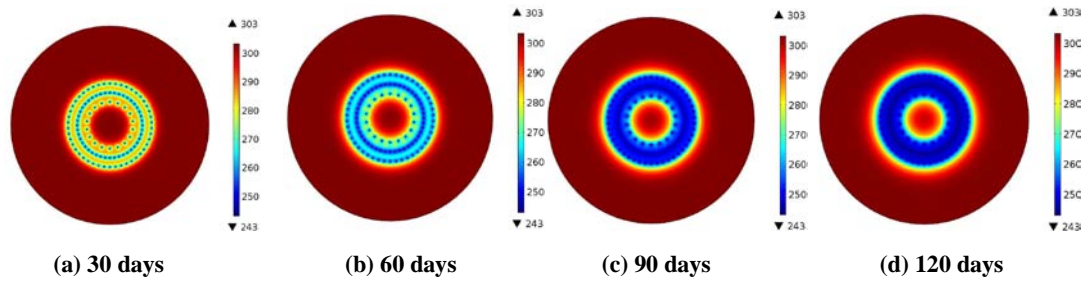


Fig. 4 Temperature fields of the frozen soil wall at different freezing durations

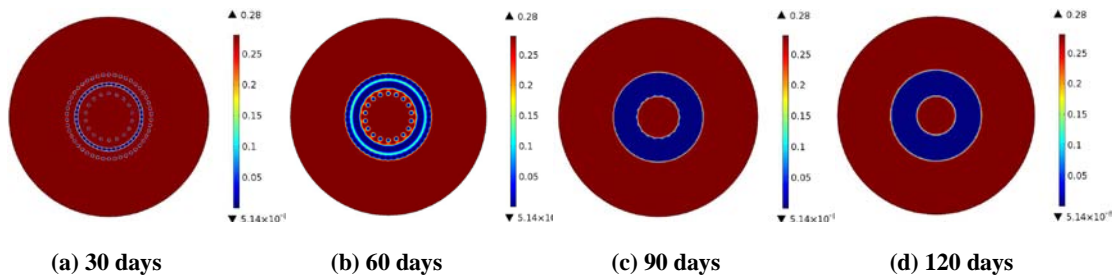


Fig. 5 Unfrozen water content fields of the frozen soil wall at different freezing durations

The distributions of unfrozen water content and temperature along the radius direction are shown in Fig. 6 and Fig.7, respectively. After freezing 30 days, the unfrozen water content of frozen soil decreases rapidly at the middle cycle of freezing pipes. There is little unfrozen water around the freezing pipe. The thickness of frozen wall at the middle cycle of freezing pipe is about 1.6m. With the increase of freezing time, the frozen regions gradually increase. After freezing 90 days, the frozen region begins to overlap and forms a whole of frozen soil wall. The thickness of frozen soil wall increases to about 10.0m after freezing 150 days.

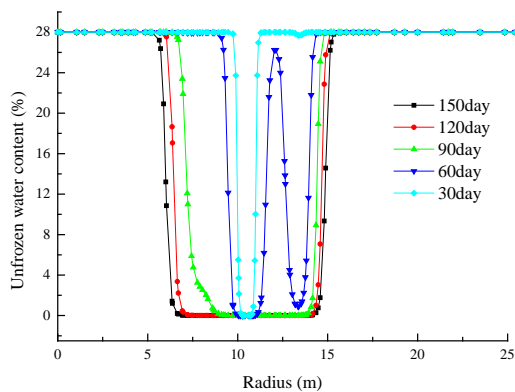


Fig. 6 Unfrozen water content distributions along radius from the center of shaft

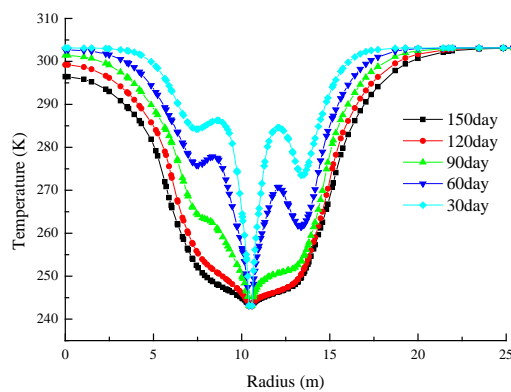


Fig. 7 Temperature distributions along radius from the center of shaft

The coefficients of thermal conductivity and specific heat capacity along radius from the center of shaft are shown in Fig. 8 and 9, respectively. The thermal conductivity and specific heat capacity of soil are greatly influenced by the freezing process. The thermal conductivity and specific heat capacity have a great change at the range of phase change. The thermal conductivity of soil is obviously improved with the decrease of temperature. However, the specific heat capacity decreases with the decrease of temperature.

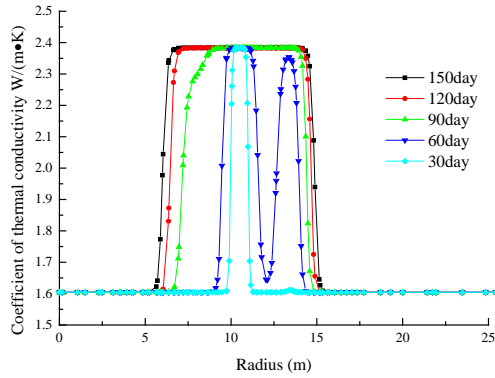


Fig. 8 Coefficient of thermal conductivity distributions along radius from the center of shaft

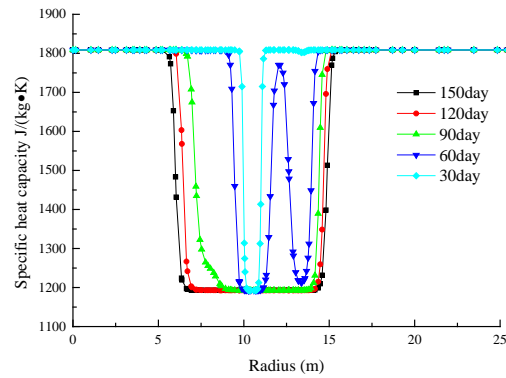


Fig. 9 Specific heat capacity distributions along radius from the center of shaft

In order to analyze the temperature evolution of frozen soil wall, the points A and B (as shown in Fig.2), which are located at the inner and outer walls, are selected as the monitoring position. The temperature evolution curves of the inner and outer walls are shown in Fig.9. The temperatures of inner and outer walls decrease monotonously with the increase of freezing time. The outer frozen soil wall is close to the outer cycle of freezing pipes. The temperature of outer wall decreases rapidly at the initial freezing stage. With the further increase of freezing time, the heat transfer in outer frozen soil wall gradually reaches a state of dynamic balance, which causes the decrease of temperature. Due to the lack of heat source in inner frozen soil wall, the temperature always decreases rapidly with the increase of freezing time.

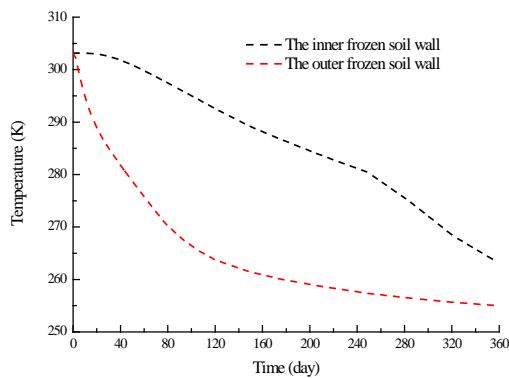


Fig. 9 Temperature variation of frozen soil wall

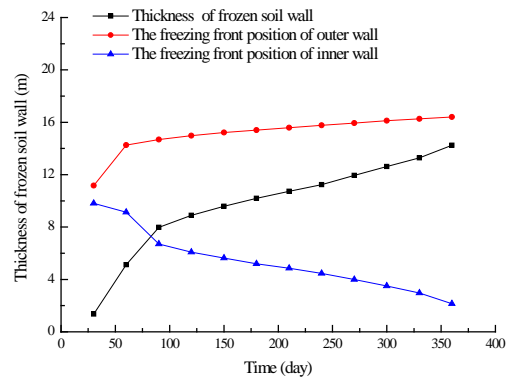


Fig. 10 Thickness of the frozen wall

The thickness and freezing front position of frozen soil wall are shown in Fig.10. The thickness of frozen soil wall increases with the increase of freezing time. It increases rapidly at initial freezing stage. Then the increasing rate of thickness gradually decreases with increase of freezing time. The evolution of inner freezing front is slow and steady. The growth of thickness is mainly due to the evolution of outer freezing front. After freezing 250

days, the thickness of frozen soil wall can increase to about 11.0m. The artificial freezing method is applicative to form a sustainable and stable waterproof wall.

Conclusions

The radius of frozen cylinder continuously increases at initial freezing stage. Then the frozen cylinders in every freezing cycle begin to overlap and a closed frozen soil wall is formed. The distribution of unfrozen water content is greatly affected by the freezing front, and there is an obvious change at the freezing front. When the temperature is below the low limit of phase change, the distribution of unfrozen water content reaches a relative stability state. The thickness of frozen soil wall gradually increases and the temperature continuously decreases with the increase of freezing time. The thickness increases to about 10.0m after freezing 150 days. After freezing 250 days, the thickness of frozen soil wall increases to about 11.0m.

Acknowledgements

This research was supported by National Natural Science Foundation of China (51574219; 41871063; 51778004); the State Key Research Development Program of China (2016YFC0600705).

Nomenclature

C_s —specific heat of soil particle, [KJ/ (kg °C)]
 C_w —specific heat of water, [KJ/ (kg °C)]
 θ_i — ice content, [-]
 θ_w —water content, [-]

References

- [1] Alireza, A., Hirokazu, A., Artificial ground freezing application in shield tunneling, *Japanese Geotechnical Society Special Publication*, 3 (2015), 2, pp. 71-75
- [2] Pimentel, E., *et al.*, Numerical interpretation of temperature distributions from three ground freezing applications in urban tunneling, *Tunnelling and Underground Space Technology*, 28 (2012), 3, pp. 57-69
- [3] Xue, Y., *et al.*, Evaluation of the Non-Darcy Effect of Water Inrush from Karst Collapse Columns by Means of a Nonlinear Flow Model, *Water*, 10 (2018), 9, pp. 1234
- [4] Klein, J., Present State of Freeze Shaft Design in Mining, *Developments in Geotechnical Engineering*, 32 (1981), 1, pp. 147-153
- [5] Wang, T., *et al.*, Stochastic analysis of uncertain thermal parameters for random thermal regime of frozen soil around a single freezing pipe, *Heat and Mass Transfer*, 54 (2018), 9, pp. 2845-2852
- [6] Li, F. Z., Xia, M. P., Study on analytical solution of temperature field of artificial frozen soil by exponent-integral function, *Journal of Southeast University*, 34 (2004), 4, pp. 469-473
- [7] Hu, X. D., Zhang, L.Y., Analytical solution to steady-state temperature field of two freezing pipes with different temperature, *Journal of Shanghai Jiaotong University*, 18 (2013), 6, pp. 706-711

- [8] Hu, K., *et al.*, Experimental Research on Multi-Circle Freezing Temperature Field for Thick Top Soil, *Journal of Mining and Safety Engineering*, 27 (2010), 2, pp. 149-153
- [9] Xue, Y., *et al.*, An elastoplastic model for gas flow characteristics around drainage borehole considering post-peak failure and elastic compaction, *Environmental Earth Sciences*, 77 (2018), 19, pp. 669
- [10] Wang, Y. S., *et al.*, Numerical Back Analysis and Simulation of Temperature Field for Shaft Sinking with Artificial Ground Freezing Method, *Journal of China University of Mining and Technology*, 34 (2005), 5, pp. 626-629
- [11] Watanabe, K., Masaru, M., Amount of unfrozen water in frozen porous media saturated with solution, *Cold Regions Science and Technology*, 34 (2002), 2, pp. 103-110
- [12] Zhou, Y., Zhou, G. Q., Analytical solution for temperature field around a single freezing pipe considering unfrozen water, *Journal of China Coal Society*, 37 (2012), 10, pp. 1649-1653
- [13] Wang, Q., *et al.*, Numerical Simulation for Soil Temperature Field of Oil Pipeline in Ground Freezing, *Journal of Guangdong University of Petrochemical Technology*, 20 (2011), 1, pp. 25-29
- [14] Zhou, X. H., *et al.*, Simultaneous measurement of unfrozen water content and ice content in frozen soil using gamma ray attenuation and TDR, *Water Resources Research*, 50 (2014), 6, pp. 9630-9655
- [15] Tomasz, K., A comprehensive method of determining the soil unfrozen water curves, *Cold Regions Science and Technology*, 36 (2003), 4, pp. 71-79
- [16] Qin, Y. H., *et al.*, A formula for the unfrozen water content and temperature of frozen soils, *Cold Regions Engineering*, 3 (2009), 1, pp. 155-161
- [17] Li, D. Q., *et al.*, The impact of unfrozen water content on ultrasonic wave velocity in frozen soils, *Procedia Engineering*, 143 (2016), 1, pp. 1210-1217

Paper submitted: May 19, 2018

Paper revised: June 28, 2018

Paper accepted: August 20, 2018